



Anal. Bioanal. Chem. Res., Vol. 9, No. 4, 411-429, September 2022.

Simultaneous Electrochemical Determination of Ascorbic Acid, Dopamine, and Uric Acid in a Variety of Food, Pharmaceutical, and Biologic Samples Using a Modified Glassy Carbon Electrode with Sunset Yellow

Hanieh Ghanbari^a, Mansour Arab Chamjangali^{a,*} and Mohammad Faraji^b

^a*Department of Chemistry, Shahrood University of Technology, Shahrood, P. O. Box: 36155-361, Iran*

^b*Department of Food Science & Technology, Standard Research Institute, Karaj, Iran*

(Received 21 March 2022, Accepted 16 June 2022)

The glassy carbon electrode (GCE) was modified with sunset yellow (SY) food dye to develop a simple, environmentally friendly, low-cost electrochemical sensor. The electrode's performance as a helpful sensor was demonstrated in the simultaneous and selective measurement of ascorbic acid (AA), dopamine (DA), and uric acid (UA). The SY dye was covalently fixed on the electrode surface. The structure and morphology of the modified electrode were investigated by scanning electron microscopy (SEM), and the results showed that SY particles were located on the surface of the GC electrode. The electrochemical activity of the modified electrode was measured using cyclic voltammetry (CV), chronoamperometry, chronocoulometry, and impedance spectroscopy (EIS) techniques. The results showed that under optimal conditions, the SY/NaOH-treated-GCE has good electrocatalytic activity, a suitable linear range (7-320, 0.2-45, 0.2-50 μM), a low detection limit (4.78, 0.12, 0.12 μM) for AA, DA, and UA, respectively, and high stability. Analytical application of SY/NaOH-treated-GCE was successfully evaluated to determine AA, DA, and UA in bell pepper, grapefruit, dopamine ampoule, vitamin C tablet, tap water, and biological samples (human blood and urine). The results reported by our team show that the SY/NaOH-treated-GCE is suitable for simultaneous and selective determination of electroactive species in various biologic and pharmaceutical samples.

Keywords: Sunset yellow, Ascorbic acid, Dopamine, Uric acid, Electrochemical sensor, Modified glassy carbon electrode

INTRODUCTION

Ascorbic acid (AA), an antioxidant that plays an essential role in the oxidation and reduction processes in the human body [1-4], is necessary for the formation of collagen in the body [5] and helps absorb iron [6,7]. AA is mainly used to treat Scorbut [8,9], kidney disease [10,11], and immune enhancement against diseases [12,13]. The recommended limit for this compound in the diet is about 30.0 to 40.0 mg per day [14]. Some studies have shown that ascorbic acid concentrations in the blood plasma of diabetic patients are lower than those of healthy people, so measuring ascorbic acid concentrations in the blood is vital to diagnose diabetes

[15,16]. Dopamine (DA), as a catecholamine, is a neurotransmitter and plays an essential role in the activity of the nervous system and hormones [17-19]. An abnormal concentration of DA in the body is a reason for diseases such as premature aging, depression, Parkinson's disease [20-22], osteoporosis, arthritis [23], schizophrenia [24], and epilepsy [25,26]. Also, a rare tumor called pheochromocytoma can increase the amount of catecholamines in the blood, causing high blood pressure, excessive sweating, headaches, palpitations, and trembles. Therefore, measuring dopamine helps detect the adrenal gland tumor called pheochromocytoma [27]. The allowed limit for DA in the blood is less than 30.0 pg ml^{-1} [28]. Uric acid (UA) is the primary source of nitrogen compounds in the urine and one of the most common compounds in the blood serum. This

*Corresponding author. E-mail: arabe51@yahoo.com

compound outcome from the final metabolism of purine in the human body [29,30]. UA normal range in the blood of men is 3.5 to 7.2 mg dl⁻¹, and in the urine is 1.48 to 4.43 mM for 24 h [31]. Irregular levels of UA lead to diseases such as ganglia [32], Lesch-Nyhan syndrome (LNS), renal disorder [33], and cardiovascular problems [34]. According to the importance and dual effects (positive and negative) of these analytes on biological materials and their potential role in the diagnosis, treatment, and prevention of diseases (biomarker effects of compounds), detection and simultaneous determination of such analytes are of interest in medical biochemistry, diagnostic, and pathological research fields.

Therefore, different analytical methods have been proposed for the simultaneous determination of these three compounds [35-43]. Among these methods, the electrochemical methods have received the greatest attention because of their simplicity, low cost, high sensitivity, high speed, and low organic solvent consumption. Voltammetric determinations of AA, UA, and DA have been widely reported due to the appropriate electrochemical properties of these compounds [44-46]. The main problem in the simultaneous determination of these compounds is the closeness of their oxidation potentials at the surface of conventional solid electrodes, which causes the overlapping of their electrooxidation peaks. Therefore, the successful simultaneous voltammetric determination of these analytes requires modifying the electrode surface. Different materials have been used to modify the surface of the electrodes, such as metal nanoparticles [47-50], nanocomposites [51-53], ionic liquids [54,55], carbon nanotubes [56,57], graphene [58-60], graphene oxide [61-63], and polymer materials [64-67].

In recent years, synthetic organic dyes have been considered in electrode modification due to their simplicity and high electrocatalytic. Some of these organic dyes are Alizarin Red [68], Methylene Blue [69], Malachite Green [70], Bromo Cresol Purple [71], Alizarin Yellow [72], and Trypan Blue (Direct Blue) [73]. Unfortunately, although these dyes have high electrocatalytic activity, they are the most important sources of water pollution [74-80]. Therefore, their use as a reactant in developing electro-analytical methods should be limited due to environmental pollution. One way to take advantage of the high electrocatalytic

activity of organic dyes without any environmental pollution is using synthetic food colorings. In addition to having high electrocatalytic activity, food colorings have advantages such as simplicity, availability, and low environmental pollution. Despite these advantages, only a few passers have been reported using food colors (such as Brilliant Blue) as the electrode modifiers [81-83]. Therefore, due to the intrinsic advantages of food colors, their use in constructing modified electrodes with desirable stability is of interest in the electro-analytical research field.

In this study, for the first time, the glassy carbon electrode (GCE) was modified using Sunset Yellow (SY) as a cheap, available, environmentally friendly, and eatable food dye. The modifier was immobilized on the surface of GCE through electro-immobilization through covalent bonding by the simple cyclic voltammetric (CV) method. According to our knowledge, there is no report on modifying the GCE surface with SY dye. The GCE modified by Sunset Yellow (SY/NaOH-treated-GCE) was used to measure AA, DA, and UA simultaneously. The modified electrode shows the separation of peaks, high stability, low detection limit, and suitable linear range. Analytical performances of the modified electrode were studied by detecting ascorbic acid, dopamine, and uric acid in various real samples such as; bell peppers, grapefruit, city water, dopamine injection, human serum, and urine. The results showed ethical recovery values.

REAGENTS AND SOLUTIONS

Ascorbic acid (AA), Dopamine hydrochloride (DA), and Uric acid (UA) were purchased from Merck. Sunset Yellow FCF (90%) dye (SY) was purchased from Sigma-Aldrich. Other reagents include citric acid, sodium citrate, sodium hydroxide, potassium chloride, potassium ferrocyanide, potassium ferricyanide, sulfuric acid, hydrochloric acid, potassium dihydrogen phosphate, and disodium phosphate, which were purchased from credible companies. All reagents were analytical grade and were used without additional purification. Doubly distilled water was used for the preparation and dilution of all solutions.

Phosphate buffer solutions (PBS) in the pH range of (4.0-8.0) were prepared by mixing appropriate volumes of 0.10 M KH₂PO₄ and Na₂HPO₄ with hydrochloric acid. Citrate buffer

solutions (CBS) at different pHs (4.0-8.0) were prepared by mixing appropriate volumes of 0.10 M citric acid, sodium hydroxide, and hydrochloric acid and adjusting the pH using the pH meter.

A 100.0 ml of $10.0 \times 10^{-3} M$ SY stock solution was prepared by dissolving 0.502 g of SY in a 100.0 ml volumetric flask. The diluted SY solutions with different concentrations were daily prepared by appropriate diluting of known required volumes of the stock solution.

A 100.0 ml stock solution of $1.0 \times 10^{-3} M$ UA was prepared by dissolving 0.0168 g of UA in a 100.0 ml volumetric flask.

A $1.0 \times 10^{-3} M$ stock solution of DA was prepared by dissolving 0.0189 g of dopamine hydrochloride in a 100.0 ml volumetric flask. The stock solution of AA with a concentration of $1.0 \times 10^{-3} M$ was prepared by solving 0.0176 g of AA in a 100.0 ml volumetric flask. Due to the low stability of AA acid and DA solutions, the stock solutions should be prepared daily. Dilute solutions of AA, DA, and UA with different concentrations were prepared by diluting the appropriate volumes of corresponding stock solutions.

100.0 ml of the 2.00 M sodium hydroxide solution and 0.10 M hydrochloric acid solution were prepared and standardized through the appropriate methods [84]. Dilute solutions were prepared daily by suitable dilution .

Sample Preparation

The fresh bell pepper and grapefruit samples were obtained from the local market. 85.00 g of bell pepper was finely ground with a mechanical grinder, and then the pepper juice was extracted by hand pressure and filtered with a filter paper (Whatman No 1). After that, the pH of pepper juice was adjusted to 5.0 using the CBS and centrifuged for 5 min at 4000 rpm. The resulting solution was decanted and transferred entirely to a 250.0 ml volumetric flask. The solution was diluted to the mark with distilled water, and 2.0 ml of the clear solution was used for electrochemical analysis.

The fruit juice of 120.0 g of grapefruit sample was collected using a mechanical juicer. The resulting juice was filtered using filter paper (Whatman No: 1). The pH of the solution was adjusted to 5.0 using CBS. The solution was centrifuged at 4000 rpm for 5 min. The resultant solution was decanted and put into a volumetric flask with a capacity of

250.0 ml. The solution was diluted to the mark with distilled water, and 2.0 ml of the clear solution was used for electrochemical analysis.

The biological samples (urine and blood serum) were taken from a healthy helper in our laboratory. A 10.0 ml urine sample was diluted 1000-fold, and 1.0 ml of the diluted sample was used for electrochemical determination. In the blood serum sample preparation, 5.0 ml of blood serum sample was centrifuged for ten minutes at 4000 rpm. The centrifuged solution was separated and diluted 100-fold. Precisely 1.0 ml of the resultant solution was used for electrochemical analysis.

The pharmaceutical samples, including dopamine ampules and Vitamin C tablets, were purchased from a local drugstore. 1.0 ml of dopamine ampule with a certified concentration of 200 mg per 5.0 ml was diluted 10000-fold with distilled water. Precisely 1.0 ml of the resultant solution was used for electrochemical analysis. Five vitamin C tablets (500 mg AA per tablet) were entirely crushed by hand mill. Then one-fifth of the powder obtained, weighing 4.1230 g was taken and dissolved in a 50.0 ml volumetric flask with distilled water. 1.0 ml of the solution was diluted 100-fold, and 1.0 ml of the resultant solution was used for analysis.

Apparatus

Electrochemical measurements were performed by a Metrohm 746 VA trace analyzer with a 747 VA stand. The three-electrode system consisted of a modified GCE (GCE/SY) working electrode, an Ag/AgCl (KCl 3.0 M) reference electrode, and a Pt wire auxiliary electrode. They were used for controlled potential electrochemical measurements. All potentials were measured and reported versus the Ag/AgCl reference electrode. GCE was purchased from Azar Electrode Company with a geometrical area of 2.0 mm. pH measurements were performed using a pH meter (Metrohm Model 780) equipped with a combined saturated calomel electrode (SCE)/glass membrane electrode. The reagents were weighed using a digital balance (Sartorius, Model A200S). A universal centrifuge (Hakim Azma Tajhiz Company) was used to centrifuge the sample solutions.

Preparation of Sunset Yellow Modified Glassy Carbon Electrode (SY/NAOH-treated-GCE)

At first, the surface of the GCE was mechanically

polished using a slurry of alumina powder (with an average particle size of 0.05 μm) on the surface of the electrode polishing plate to achieve a glossy surface. Then, 10.0 ml of 1.0 mM SY solution containing 0.20 M NaOH was transferred to the electrochemical cell. The GCE was then placed in the electrochemical cell, and 20 successive potential cyclings were performed in the range of -0.5 to +1.5 V with a scan rate of 100 mV s^{-1} using the cyclic voltammetry (CV) technique. The modified electrode was washed twice with distilled water to remove any impurities from its surface. Then, the modified electrode was placed in a 0.20 M NaOH solution, and an additional five successive potential cyclings were applied using the CV technique at the above-mentioned instrumental conditions. This further potential cycling removes the unreacted SY monomers from the electrode surface, and the modified electrode creates a stable electrochemical response.

Analytical Procedure

For differential pulse voltammetry (DPV) measurement, an aliquot volume of standard or sample solution containing known amounts of AA, DA, and UA as analytes was transferred into the electrochemical cell. Then, 4.0 ml of CBS at $\text{pH} = 5.0$ was added, and the solution was diluted up to 10.0 ml using distilled water. Then, the DP voltammogram of the solution was recorded by applying a positive-going potential scan in the potential range of -0.10 to 0.70 V with the potential scan rate of 60 $\text{mV}\cdot\text{s}^{-1}$ and a pulse amplitude of 60 mV. The peak currents for AA, DA, and UA (i_s) oxidation were measured at the peak potentials of -0.10, 0.30, and 0.47 V, respectively. Also, the DP voltammogram for the blank solution was recorded under the same conditions. The currents at the potentials of 0.10, 0.30, and 0.47 V were recorded and used as the background current (i_b) to calculate the analytical signal ($\Delta i = i_s - i_b$). The analytical signals (Δi) at the corresponding peak potentials were used to construct calibration curves for the quantitative determination of analytes. After each measurement, the modified electrode was cleaned by twice washing with distilled water; then, the electrode surface was thoroughly reactivated in 0.2 M NaOH solution by five consecutive CV potential cycling in the potential range of -0.5 to 1.5 V with a scan rate of 100 mV s^{-1} .

RESULTS AND DISCUSSION

Immobilization of SY on the Surface of GCE

Figures 1a and 1b show the successive cyclic voltammograms recorded in the modification of the GCE

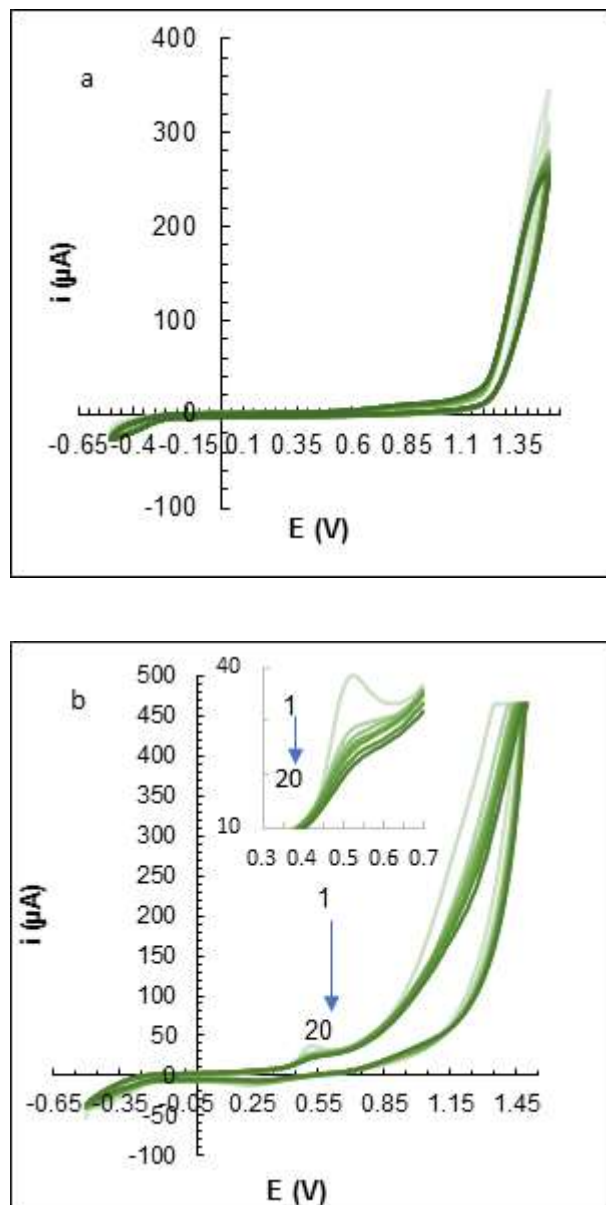


Fig. 1. Cyclic voltammograms (20 cycles) for a: NaOH-treated-GCE, and b: SY/NaOH-treated-GCE. Inset is locally-amplified cyclic voltammograms. Conditions: $1.0 \times 10^{-3} \text{ M}$ of SY in 0.20 M NaOH, the scan rate of 100 mV s^{-1} .

surface in the 0.2 M NaOH solution (NaOH-treated-GCE) and the mixed solution containing 0.2 M NaOH solution and $1.0 \times 10^{-3} M$ SY (SY/NaOH-treated-GCE). No redox peak was observed in the cyclic voltammograms of the GC electrode surface when treated with NaOH (Fig. 1a).

However, an oxidation peak at a potential of 0.54 V is observed in GCE modification using NaOH and SY mixed solution, related to SY oxidation. The oxidation peak current of the SY decreases with the increasing number of cycles. This is probably associated with the covalent formation of the SY film on the GCE surface through the formation of the cationic radicals [85,86] (Scheme 2).

The anodic scan of SY in an aqueous medium can cause radical cation formation (Scheme 2). The azo-SY group becomes a radical cation with the loss of one electron. A covalent bond is probably formed between the nitrogen group of the SY and the sp^2 carbon of the GC electrode. The results are consistent with previous work for covalently stabilizing other modifiers on the GCE surface using the cyclic voltammetric technique [85-91].

Characterizations of SY-Modified Electrodes (SY/NaOH-treated-GCE)

The morphology of the electrode surface was studied using the recorded FESEM images. As shown in Fig. 2a, the surface of the unmodified GCE is uneven and non-uniform. While the surface of SY/NaOH-treated-GCE has become uniformly rougher, it shows that the SY modifier is immobilized at the surface of the SY/NaOH-treated-GCE (Fig. 2b).

Electrochemical Impedance Studies

Electrochemical impedance spectroscopy (EIS) is an efficient method to evaluate the resistance of the electrode surface against charge transfer. The effect of electrode modification on charge transfer resistance was investigated by immersing both modified and unmodified GC electrodes in a solution containing 5.0 mM $[Fe(CN)_6]^{4-}$ and 0.10 mM KCl and recording EI spectrum. The recorded Nyquist plots and equivalent circuits are shown in Fig. 3. In the designed equivalent circuit (Fig. 3I), R_s , R_{ct} , and C are the solution resistance, charge transfer resistance, and double layer capacitance, respectively. Z_w is related to semi-finite linear diffusion. Both electrode Nyquist diagrams (Fig. 3) consist

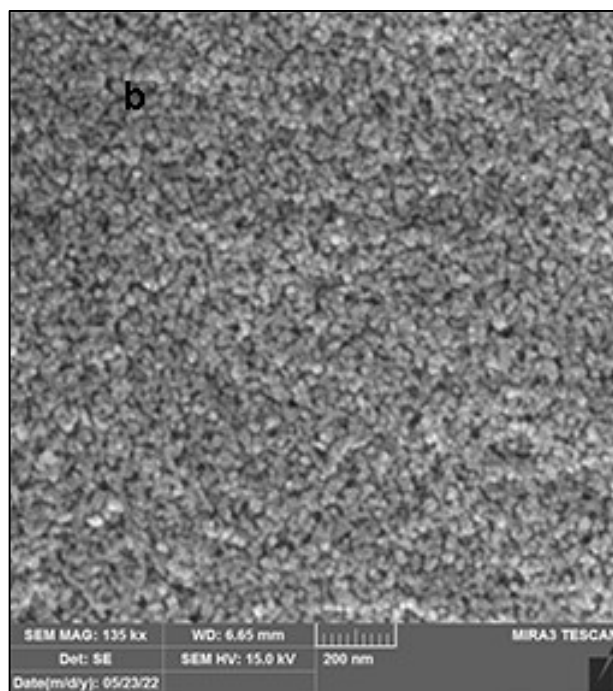
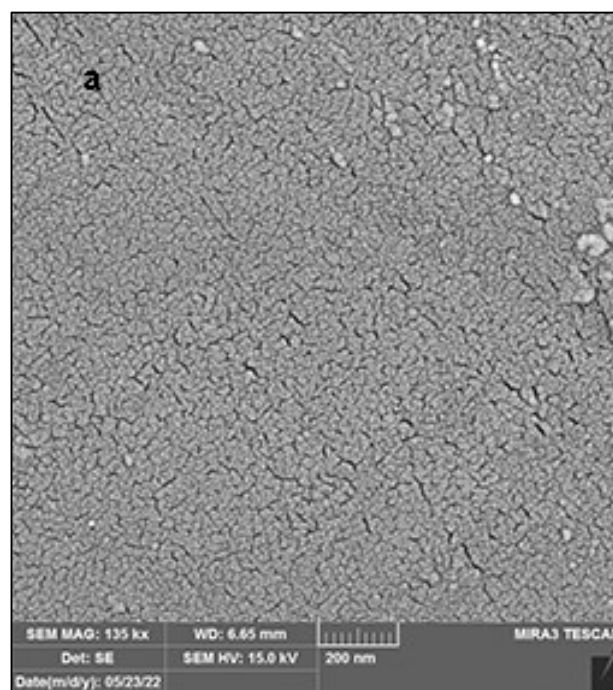


Fig. 2. SEM images of (a): bare GCE, and (b): SY/NaOH-treated-GCE.

of two parts, the linear part related to the diffusion-controlled process and the semi-circular part associated with the

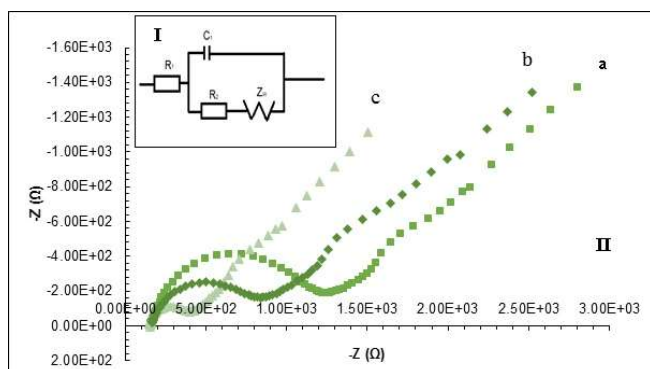
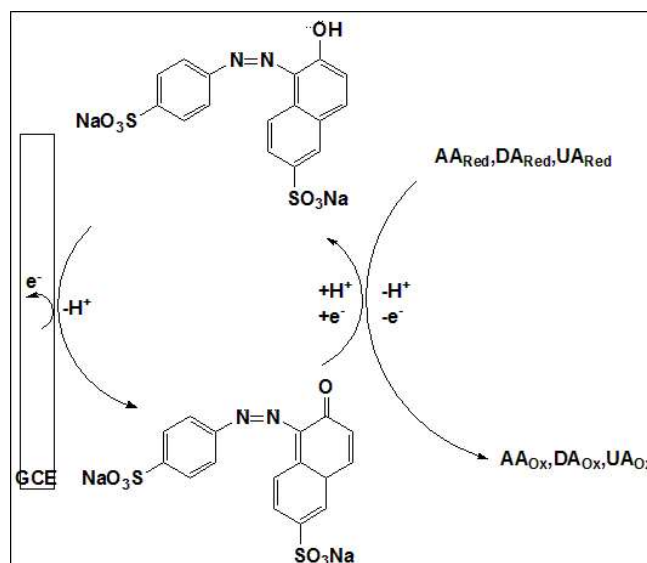


Fig. 3. Electrochemical impedance spectra for bare GCE (a), NaOH-treated-GCE (b), and SY/NaOH-treated-GCE (c). The inset shows the equivalent circuit. R_1 is solution/electrolyte resistance, R_2 is charge-transfer resistance, Z_w is Warburg impedance related to semi-infinite linear diffusion, and C_1 is double-layer capacitance.

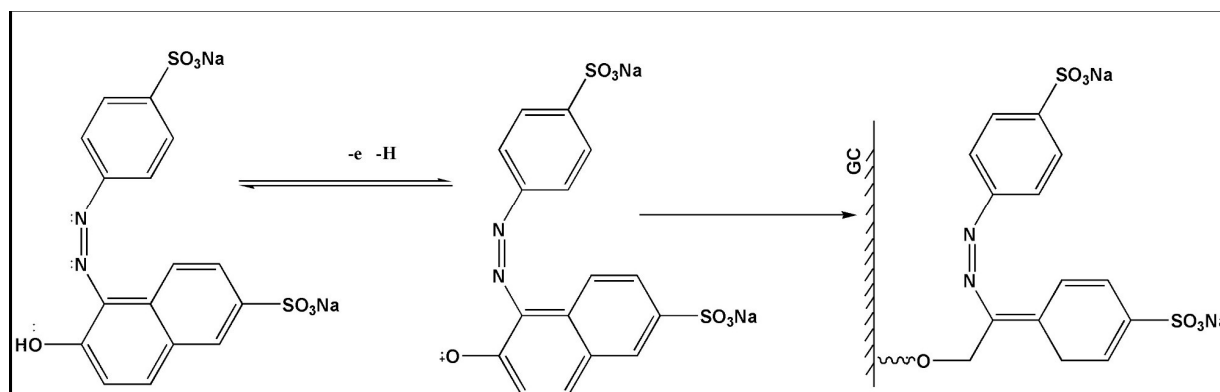
electron transfer process. The diameter of the semi-circular section indicates charge transfer resistance (R_{ct}). According to the results obtained (Fig. 3II), the smaller diameter of the semi-circle in the Nyquist plot of the modified electrode (SY/NaOH-treated-GCE) indicates lower charge transfer resistance and easier electron transfer on the surface of the SY/NaOH-treated-GCE compared to the GCE-treated and bare GCE. After data processing with Ivium software, the values of 9.80×10^2 , 6.45×10^2 and $2.14 \times 10^2 \Omega$ were calculated for R_{ct} of the bare GCE, NaOH-treated-GCE, and SY/NaOH-treated-GCE, respectively. The less R_{ct} in



Scheme 1. The proposed electrocatalytic mechanism for the oxidation of AA, DA, and UA on the surface of the SY/NaOH-treated-GCE

SY/NaOH-treated-GCE indicated that the SY film on SY/NaOH-treated-GCE accelerated the electron transfer process according to the electrocatalytic mechanism suggested in Scheme 1.

The active surface area of modified and unmodified electrodes were calculated using the chronoamperometry technique via the Cottrell equation under the diffusion-controlled condition [92]. For this purpose, the modified and unmodified electrodes were placed in the solutions with different concentrations of $[\text{Fe}(\text{CN})_6]^{4-}$ containing 0.10 M



Scheme 2. Proposed mechanism for modification of GCE with SY

KCl, and the chronoamperograms were recorded at the applied potential of 0.35 V. The results are shown in Figs. 1S-3S (Supplementary). The chronoamperograms of a blank solution (containing only 0.10 mM KCl) were also recorded. After making point-to-point corrections for the blank, the graphs of current versus $t^{1/2}$ at different concentrations of $[\text{Fe}(\text{CN})_6]^{4-}$ were drawn for bare GCE, NaOH-treated-GCE, and SY/NaOH-treated-GCE (inset of Figs 1S-3S). According to the Cottrell equation, the obtained graphs (I vs. $t^{1/2}$) are linear with slopes of $nFAD^{1/2}\pi^{1/2}$. The slopes are dependent on the concentration of $[\text{Fe}(\text{CN})_6]^{4-}$, therefore, the slopes of the resulting straight lines were plotted vs. $[\text{Fe}(\text{CN})_6]^{4-}$ concentrations. The following equations were obtained:

$$\text{GCE: slope} = 3.970C - 1.450 \quad (R^2 = 0.9775) \quad (1)$$

$$\text{NaOH-treated-GCE: slope} = 5.534C - 0.620 \quad (R^2 = 0.987) \quad (2)$$

$$\text{SY/NaOH-treated-GCE: slope} = 6.259C - 1.293 \quad (R^2 = 0.998) \quad (3)$$

Based on the results, with $n = 1$ and $D = 6.5 \times 10^{-6} \text{ cm}^2 \text{ s}^{-1}$ for $[\text{Fe}(\text{CN})_6]^{4-}$ in 0.10 M KCl, the active surface areas were calculated to be 0.029, 0.04, and 0.045 cm^2 for the bare GCE, NaOH-treated-GCE, and SY/NaOH-treated-GCE, respectively. The results showed that the electrochemical effective surface area of the electrode is larger after modification with SY, demonstrating that SY increases the electrochemical effective surface area of the electrode; consequently, it increases the oxidation peak current.

The amount of the SY as a modifier on the electrode surface is a crucial parameter and should be studied when the electrode is chemically modified. Therefore, the chronocoulometry technique was chosen to quantify SY concentration on the GC electrode surface. For this purpose, SY/NaOH-treated-GCE was placed in a PBS solution (pH = 5.0) containing 30.0 μM DA, and the chronocoulogram was recorded by applying a sufficiently positive potential step of 0.5 V (more positive than the potential of SY). The chronocoulograms at the surfaces of bare-GCE and SY/NaOH-treated-GCE were also recorded. The following

equation shows the relationship between Q and time in the presence of surface adsorbed species [93].

$$Q_{\text{total}} = \frac{2nFAC_oD_o^{1/2}}{\pi^{1/2}} \cdot t^{1/2} + Q_{\text{ads}} + Q_{\text{dl}} \quad (4)$$

where Q_{dl} is the double layer charge (C), Q_{ads} is the adsorption charge (C), F is the Faraday constant (C mol^{-1}), A is the surface area of the electrode (cm^2), n is the number of electrons exchanged, C_o is the concentration of ox species (M), and D_o the diffusion coefficient of ox species ($\text{cm}^2 \text{ s}^{-1}$). According to Eq. (1), the graph of Q vs. $t^{1/2}$ for Q-t data of SY/NaOH-treated-GCE in the sample solution is linear with the intercept of $Q_{\text{ads}} + Q_{\text{dl}}$. On the other hand, assuming the absence of electroactive species at the bare-GCE surface does not affect the structure of the electrode surface double layer, the Q_{dl} term could compensate by point-by-point subtraction of the Q-t data of bare-GCE in blank solution from the Q-t data of SY/NaOH-treated-GCE in DA solution. Therefore, after correcting Q-t data of SY/NaOH-treated-GCE immersed in DA solution relative to blank data, the graph of Q vs. $t^{1/2}$ was drawn (Fig. 4S). The intercept of the linear Q - $t^{1/2}$ diagram is equal to Q_{ads} and was found as $0.1652 \times 10^{-6} \text{ C}$. The concentration of electroactive species at the modified electrode surface (Γ) was calculated using the equation $Q_{\text{ads}} = nF\Gamma A$ [93,94]. By taking the values of $n = 1$, $A = 0.045 \text{ cm}^2$ for SY/NaOH-treated-GCE, and the defined value for F, the surface concentration of the SY (Γ) on SY/NaOH-treated-GCE was estimated to be $3.8 \times 10^{-11} \text{ (mol cm}^{-2}\text{)}$.

The electrons and protons involved in the redox process of the SY film modifier were investigated using the dependence of the peak potential of SY oxidation on the pH. Therefore, the effect of pH on SY oxidation peak potential (E_p) was investigated by cyclic scanning of the potential in the range of -0.3 to 1.0 V at a scan rate of 200 mV s^{-1} when SY/NaOH-treated-GCE was immersed in phosphate buffer solutions with different pH values in the range of 3.0-8.0. The recorded CVs are shown in Fig. 4. The results show a redox peak at different pHs, confirming that the SY film is electroactive in the studied range. Additionally, at pH ranges of 3.0-8.0, with increasing pH, the potential of the SY redox peak shifts towards negative values. These observations

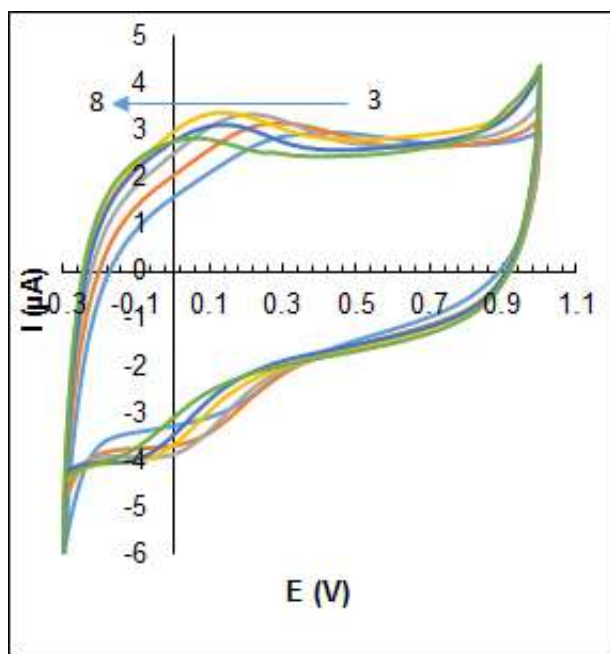


Fig. 4. Cyclic voltammograms of SY/NaOH-treated-GCE in PBS solution pH = (3.0, 4.0, 5.0, 6.0, 7.0, 8.0) at scan rate 200 mV s^{-1} .

confirm that the reaction is associated with proton transfer [95-97]. As illustrated in the inset of Fig. 5S, the linear relationship between the SY anodic peak potential (E_{pa}) and pH can be expressed with the equation of $E_{pc}(\text{V}) = 0.0586\text{pH} + 0.5205$ ($R^2 = 0.9959$). The slope obtained is close to the theoretical Nernst slope (0.0592 V); therefore, the number of exchanged electrons and protons in the electrochemical redox process of surface adsorbed SY is equal. According to the proposed mechanism in Scheme 1, the transfer process involves one proton and one electron.

The electrochemical behavior of SY on the SY/NaOH-treated-GCE surface was investigated using the CV technique at different scan rates. For this purpose, cyclic voltammograms of SY/NaOH-treated-GCE were recorded in PBS with pH = 5.0, in the potential range of -0.3 to 1.0 V with scan rates of 50-250 mV s^{-1} (Fig. 5). The diagrams of anodic peak currents (I_{pa}) vs. the scan rate were plotted (Fig. 6S). The results show that I_{pa} increases linearly with increasing scan rates (linear I vs. v), indicating that the current of species is surface controlled [98]. Also, the I_{pa}/I_{pc} is approximately equal to one. On the other hand, the potential

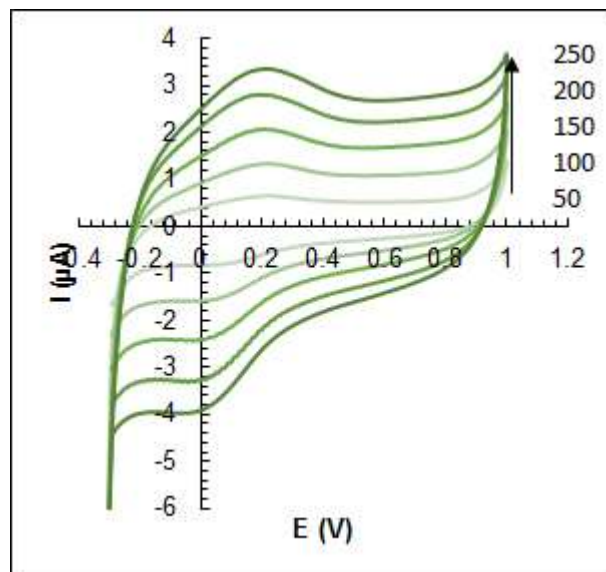


Fig. 5. Cyclic voltammograms of SY/NaOH-treated-GCE in PBS solution of pH = 5.0 at different scan rates. (50, 100, 150, 200 and 250 mV s^{-1}).

difference between anodic and cathodic peaks ($E_{pa} - E_{pc}$) is more significant than $59/n$ (mV) and increases linearly with increasing scan rate. Besides, the E_{pc} potential shifts negatively as the scan rate increases. These results confirm that the modifier reaction at the electrode surface is quasi-reversible [99,100].

The DPV technique was used to investigate the electrochemical responses of AA, DA, and UA on bare GCE, NaOH-treated-GCE, and SY/NaOH-treated-GCE. The DP voltammograms of bare GCE, NaOH-treated-GCE, and SY/NaOH-treated-GCE, in CBS pH = 5.0 containing 100.0, 5.0, and 10.0 μM of AA, DA, and UA, respectively, are shown in Fig. 6. Due to the slow electron transfer process at the bare GCE surface, the oxidation peaks of AA, DA, and UA are very weak, wide, and asymmetric at potentials of 0.13, 0.31, and 0.47, respectively (Fig. 6a). However, at the NaOH-treated-GCE (Fig. 6b), the oxidation peaks of all three analytes are well separated (0.11 V, 0.30 V, and 0.47 V for AA, DA, and UA, respectively). Moreover, the analytes signals are enhanced due to the improved active surface area of NaOH-treated-GCE (0.040 cm^2 for NaOH-treated-GCE compared with 0.029 cm^2 for SY/NaOH-treated-GCE). According to Fig. 6c, the anodic peak potentials (E_{pa}) of AA,

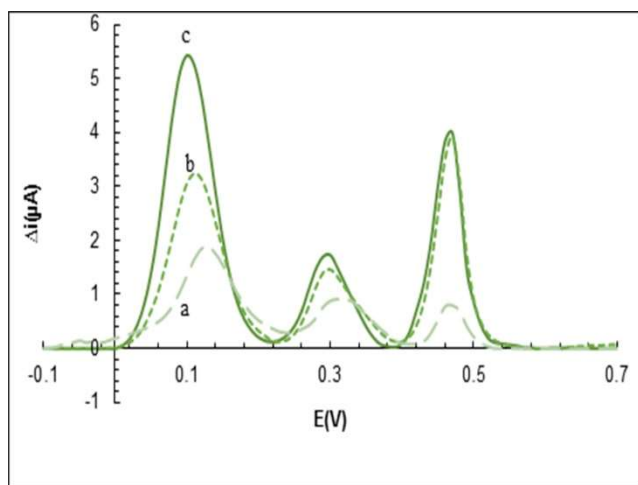


Fig. 6. DP voltammograms of the 300.0 μM AA, 5.0 μM DA, and 10.0 μM UA at bare GCE (a) NaOH-treated GCE (b) and SY/NaOH-treated-GCE (c) in PBS pH = 5.0.

DA, and UA were observed at 0.09 V, 0.29 V, and 0.46 V, respectively, at the surface of the SY/NaOH-treated-GCE. The observed peak potentials are lower than the corresponded anodic peak potentials at NaOH-treated-GCE, and the oxidation currents are enhanced in the presence of SY at the electrode surface. With these results and the fact that the surface areas of NaOH-treated-GCE (0.040 cm^2) and SY/NaOH-treated-GCE (0.045 cm^2) are nearly equal, it can be concluded that the SY, as a modifier, facilitates the rate of electron transfer at the SY/NaOH-treated-GCE. In addition, the peak potential difference of the analytes in the SY/NaOH-treated-GCE is more significant, which indicates a better peak separation in the presence of SY as a modifier. However, the results confirm that the SY is an appropriate modifier for constructing a sensitive electrochemical sensor for the simultaneous determination of AA, DA, and UA.

Optimization of Experimental Conditions

Optimization of modified electrode construction conditions. During the electrode modification process, an electrolyte is used as a reaction medium to increase the conductivity, reduce the internal resistance of the solution, and eliminate the migration current. The influence of electrolyte type on the signal of the analytes was evaluated using the CV technique. Cyclic voltammograms were

recorded in solutions containing SY (1.0 mM) and 0.1 M of various supporting electrolytes, including; NaOH, H_2SO_4 , KNO_3 , and PBS. After that, the DP voltammograms were recorded in a solution containing a specific amount of analytes and CBS, pH = 5.0. As shown in Fig. 7S, the PBS and NaOH synthesis medium have the highest DPV signal. However, according to Table 1S, NaOH has better repeatability and less standard deviation than PBS. So, NaOH was used as a medium for synthesis to achieve better repeatability and sensitivity.

The electrolyte concentration affects the quality of the modified film by oxidizing the surface of GCE and increasing the electroactive sites. The GCE was modified to optimize supporting electrolyte concentration using the CV technique in solutions containing 1.0×10^{-3} M of SY and different concentrations (0.03-0.3 M) of NaOH. The effect of electrolyte concentration on the electrochemical response was then investigated using DPV in a solution containing a known concentration of analytes and CBS with a pH of 5.0. As shown in Fig. 8S, with increasing electrolyte concentration up to 0.2 M, the analyte signal increases and subsequently decreases. Increased NaOH concentration causes oxidation of the electrode surface, an increase in electroactive sites, and the functional groups (hydroxyl, carbonyl, and carboxyl) formation, which leads to an increase in the peak current of analytes [101]. However, at higher concentrations of 0.2 M, the most active sites on the GC surface were oxidized, and the possibility of bond formation between the SY and the GC surface was limited. Therefore, the amount of SY on the GCE surface decreased. This problem reduced the quality of the SY film on the GC surface and ultimately reduced the analyte signal. As a result, 0.2 M was chosen as the optimal electrolyte concentration for SY/NaOH-treated-GCE modification.

The modifier amount on the electrode surface plays an essential role in the voltammetric signal of the modified electrode. Therefore, the effect of different concentrations of SY as a GC modifier on the oxidation current of analytes was studied. For this purpose, the GCE was immersed in a 0.2 M NaOH solution containing different amounts of SY (0.25×10^{-3} - 2.0×10^{-3} M). Then the GCE was modified using the CV technique with 20 potential sweeps from -0.5 to 1.5 V. Then, using the DPV technique, the signal of analytes was recorded with an applied potential of -0.3 to 0.7. As

illustrated in Fig. 9S, increasing the SY concentration from 0.25×10^{-3} to 1.0×10^{-3} M increased the signal of analytes. However, at concentrations greater than 1×10^{-3} M, increasing the thickness of the modifier layer on the electrode surface decreases electrical conductivity, hence decreasing the analyte signal [64]. As a result, 1.0×10^{-3} M was chosen as the best modifier concentration.

The thickness of the modifier film is affected by the number of voltammetric cycles. Therefore, the effect of increasing the scan number (from 10 to 30) on the voltammetric response of analytes was investigated. The obtained data indicates that when the number of cycles increases to 20, the oxidation current intensity of the analytes also increases. However, as the number of cycles exceeds 20, the oxidation current of the analyte decreases due to the increased film thickness and decreased electron transfer of the analyte at the electrode surface. As a result, 20 cycles were selected in the electrode modification process.

Optimization of simultaneous determination conditions. Using the DPV technique, the effect of pH on the electrochemical behavior of AA, DA, and UA, as well as the sensitivity of the proposed electrochemical sensor, were studied. For this purpose, the SY/NaOH-treated-GCE was placed in phosphate buffer solutions with pH values between 3.0 to 8.0, including known quantities of AA, DA, and UA. Then, the potential was scanned from -0.3 V to 1.0 V at a scan rate of 50 mV s^{-1} , and the DP voltammograms were recorded (Fig. 7). As shown in Fig. 7, as the pH increases, the anodic peak potentials (E_{pa}) of the analytes shift to negative values, which indicates the association of proton transfer in the oxidation of analytes [97,102].

As illustrated in Fig. 7, as pH rises, the anodic peak potentials (E_{pa}) of the analytes shift to negative values, indicating proton transfer in the oxidation of analytes [97,102]. The E_{pa} values of each analyte were plotted against pH for further investigation. The results (shown in Fig. 10S (a-b)) indicate a linear relationship between E_{pa} and pH for all three analytes, as demonstrated by the linear regression equations listed below:

For more investigations, the E_{pa} values of each analyte were plotted against pH. The results (shown in Fig. 10S (a-b)) show that there is a linear relationship between E_{pa} and pH for all three analytes with the below linear regression equations:

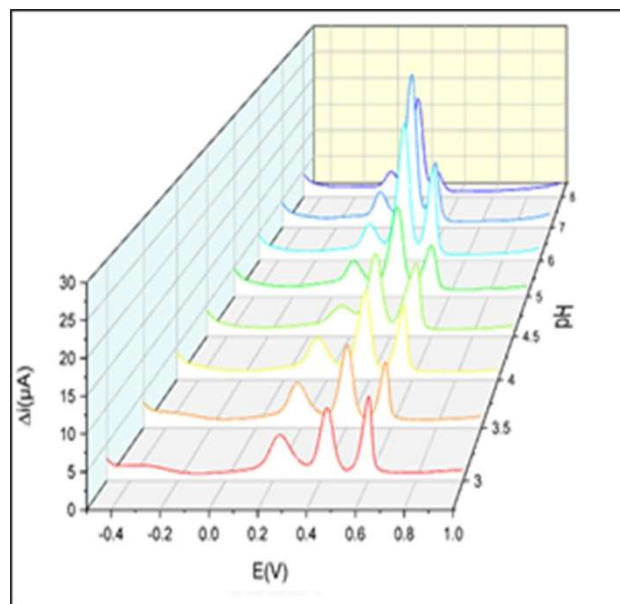


Fig. 7. DP voltammograms of a mixture of 100.0 μM AA, 20.0 μM DA, and 10.0 μM UA at SY/NaOH-treated-GCE in 0.1 M PBS of various pHs

$$\text{For AA: } E_{AA} = -0.0409pH + 0.03298 \quad (R^2 = 0.984) \quad (5)$$

$$\text{For DA: } E_{DA} = -0.0528pH + 0.5944 \quad (R^2 = 0.997) \quad (6)$$

$$\text{For UA: } E_{UA} = -0.0661pH + 0.8212 \quad (R^2 = 0.9789) \quad (7)$$

According to Eq. (5), the slope of the linear equation for AA is 0.0409, which indicates the inequality of the number of electrons and protons in the AA oxidation process; therefore, two electrons per one proton mechanism is involved. Eqs. (6) and (7) show that the slopes of E_{pa} vs. pH linear relationships for DA and UA are similar to the slope of the Nernst equation. Therefore, the number of e and protons exchanged in the oxidation of DA and UA is identical. The results are in good agreement with the previously reported results for the oxidation of AA, DA, and UA [103-105]. The effect of pH on the sensitivity (oxidation peak current) was also studied. For this purpose, the anodic peak currents of analytes were plotted versus pH (Fig. 11S). Figure 11S shows

the anodic peak currents are maximum at pH = 5.0 for AA and UA, whereas at pH = 7.0. A decrease in the anodic peak current of DA at pH values greater than 7.0 is due to the self-polymerization of DA at alkaline pH values [58,106]. Also, the highest peak separation (ΔE_p) between AA and DA and between DA and UA was observed at pH = 5.0. Thus, pH = 5.0 was selected as the optimal pH to achieve better peak resolutions and appropriate sensitivity.

In this study, the buffer solution was used as the supporting electrolyte. The nature of supporting electrolytes has an influential role in electrochemical determinations. Therefore, the effect of buffer type (supporting electrolyte) on the oxidation peak current of each analyte was investigated using acetate, citrate, phthalate, and phosphate buffer with a pH of 5.0 as supporting electrolytes. For this purpose, differential pulse voltammograms of solutions containing AA, DA, and UA with concentrations of 300.0, 10.0, and 20.0 μM , respectively, and different buffers types with the same concentration of 0.1 M and pH of 5.0 were recorded in the potential range of -0.1 to 0.7 V at the SY/NaOH-treated-GCE. According to the results obtained (Fig. 12S), the highest peak current was observed in the CBS. Hence, a 0.10 M CBS with a pH of 5.0 was used as the supporting electrolyte for the simultaneous determination of AA, DA, and UA.

The influence of the potential scan rate (v) on the anodic peak currents (i_p) of analytes was investigated. For this purpose, DP voltammograms of SY/NaOH-treated-GCE immersed in the CBS with a pH of 5.0 containing a specific analyte concentration were recorded at a potential ranging from 0.1 to 0.7 V at various scan rates, in the range of 20 to 120 mV s^{-1} . The results indicate that the analytical signal reaches its maximum value at a scan rate of 60 mV s^{-1} ; after that, it becomes nearly constant. However, the background current is also increased at high potential scan rates. So, the scan rate of 60 mV s^{-1} was selected as the optimal value for the next studies.

Since the analytical signal in the DPV technique depends on the pulse amplitude [87]. The effect of pulse amplitude on the analytical signals of analytes was investigated in the range of 10 to 80 mV. DP voltammograms of solutions containing 300.0, 10.0, and 20.0 μM of AA, DA, and UA, respectively, in the CBS with pH = 5.0 were recorded in the potential range of -0.1 to 0.7 V using different values of the

pulse amplitude. According to the obtained evidence, with increasing pulse amplitude, the peak oxidation current of the analytes increases. However, peak width also increases with increasing pulse amplitude; therefore, the peak separation decreases at a higher pulse amplitude, and the peak separations are not favorable at pulse amplitudes higher than 60 mV. Therefore, a potential pulse with an amplitude of 60 mV was selected as the optimal value for further studies.

As an effective differential pulse voltammetric parameter, the effect of pulse time was studied in the range of 10-60 ms. Under optimal conditions of other parameters, the DP voltammogram of the modified electrode was recorded in a solution containing 300.0, 10.0, and 20.0 μM of AA, DA, and UA, respectively. As shown in Fig. 13S (supplementary materials), the anodic peak currents of analytes increase with increasing pulse time up to 20.0 ms and then decrease with increasing pulse time; therefore, a pulse duration of 20.0 ms was chosen for further studies.

Analytical Parameters in the DP Simultaneous Determination of DA, AA, and UA Using SY/NaOH-Treated-GCE

The lack of synergistic effects amongst analytes when using the DPV method for the simultaneous determination of multiple analytes is crucial and should be investigated. Therefore, voltammograms of solutions containing all three analytes were recorded under optimum conditions to detect the possible synergistic effects. The solutions were made so that the concentration of one analyte remained constant in each solution while the concentrations of the other two analytes varied. According to the results (Fig. 14-17S), the peak current of the analyte with constant concentration is mainly independent of the concentration of other analytes. Furthermore, regardless of which analyte concentration was constant, the oxidation current of the analytes with various concentrations increased linearly as the concentration. These results confirm the lack of synergistic effects between the analytes. Finally, as shown in Fig. 17S, by increasing the concentration of all three analytes simultaneously, the signal of analytes increases simultaneously and linearly with a correlation coefficient of about 0.999 for all three analytes. Therefore, the results are dedicated to the possible simultaneous determination of three analytes with reliable results and the least error *via* drawing linear calibration

graphs. To obtain the linear relationships between DP oxidation peak currents and analyte concentrations, as calibration curves, DP voltammograms at the surface of GCE immersed in four different solutions with a pH of 5.0 containing different concentrations of analytes (solutions I to IV) were recorded at the optimum conditions. The obtained results for the solution I (a constant concentration of 50.0 μM for AA; different concentrations in the ranges of 5.0-25.0 μM for both DA and UA), the solution II (a constant concentration of 5.0 μM for DA; different concentrations in the ranges of 30.0-200.0 μM , and 5.0-25.0 μM for AA and UA, respectively), the solution III (a constant concentration of 5.0 μM for UA; different concentrations in the ranges of 30.0-200.0 μM , and 5.0-25.0 μM for AA and DA respectively), and the solution IV (different concentrations in the ranges of 30.0-200.0 μM , for AA 5.0-25.0 μM for both DA and UA, respectively) are shown in Fig. 18-20S. As shown in Fig. 18S, at constant AA concentrations, the oxidation peak current for AA is nearly constant, while the oxidation peak currents of DA and UA increase linearly with concentrations according to the regression equations of $i_{AA}(\mu\text{A}) = 0.0211C_{AA}(\mu\text{M}) + 0.1042$ ($R^2 = 0.9983$, $n = 3$), $i_{DA}(\mu\text{A}) = 0.786C_{DA}(\mu\text{M}) - 1.120$ ($R^2 = 0.999$, $n = 3$), and $i_{UA}(\mu\text{A}) = 0.875C_{UA}(\mu\text{M}) - 1.428$ ($R^2 = 0.999$, $n = 3$) for DA and UA, respectively. According to Fig. 19S, at constant DA concentrations, with increasing concentrations of AA and UA, the oxidation peak currents of AA and UA increase linearly (with a correlation coefficient of 0.998 for both AA and UA). In contrast, the oxidation peak current of dopamine is constant. Also, at constant UA concentration, with increasing concentrations of DA and AA, the oxidation peak currents of DA and AA increase linearly (with a correlation coefficient of 0.999 for both AA and DA), while the oxidation peak currents of UA are constant (Fig. 20S). Finally, according to Fig. 8, by increasing the concentration of all three analytes simultaneously, the analytical signals increase simultaneously and linearly with the concentration increasing. Data analysis using the least square method shows that the calibration graphs are linear in the concentration ranges of 7.0-320.0 μM , 0.2-45.0 μM , and 0.2-50.0 μM ($n = 7$) for AA, DA, and UA. The calibration curve equations for three analytes at the corresponding concentration range are as follows:

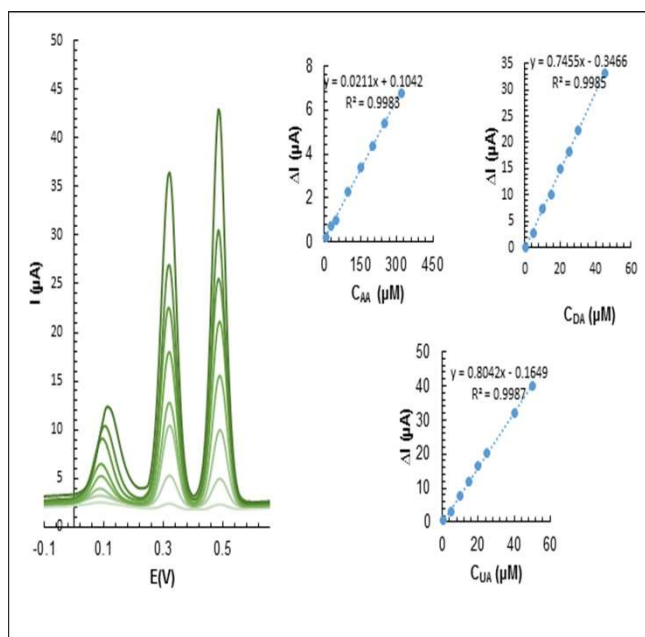


Fig. 8. DP voltammograms of SY/NaOH-treated-GCE with 0.1 M CBS (pH 5) containing different concentrations of AA (7-320 μM), DA (0.2-45 μM), and UA (0.2-50) μM . Insets are typical calibration plots of AA, DA and UA sensor.

$$i_{AA}(\mu\text{A}) = 0.0211C_{AA}(\mu\text{M}) + 0.1042 \quad (R^2 = 0.9983, n = 8) \quad (8)$$

$$i_{DA}(\mu\text{A}) = 0.7455C_{DA}(\mu\text{M}) - 0.3466 \quad (R^2 = 0.9985, n = 8) \quad (9)$$

$$i_{UA}(\mu\text{A}) = 0.8042C_{UA}(\mu\text{M}) - 0.1649 \quad (R^2 = 0.9987, n = 8) \quad (10)$$

The calculated detection limit of the proposed sensor was also estimated according to the below equation:

$$\text{LOD} = K S_b / m \quad (11)$$

K is the numerical factor chosen according to the desired confidence level and generally equals 3, S_b is the standard deviation of the blank signal, and m is the calibration curve slope. The values of S_b were calculated using the blank currents at the oxidation peak potentials of analytes by six repeated recordings of DP voltammograms for blank solution

(CBS with pH 5.0). According to the results, the S_b values of 0.033, 0.031, and 0.033 were calculated for AA, DA, and UA. By taking and calibration curve slopes (m values) of 0.021, 0.74, and 0.80 for AA, DA, and UA, respectively, and the corresponding values of S_b , the detection limit of the proposed sensor was found to be 4.78, 0.12, and 0.12 for AA, DA, and UA, respectively.

Accuracy and Precision

Three different concentrations of AA, UA, and DA were repeatedly measured within the linear range of the related calibration curves to assess the accuracy and precision of the proposed method. For this purpose, five repeated DP voltammograms of solutions containing known amounts of three analytes were recorded, and the analytical signals (Δi_p) of each analyte were extracted. The analytical signals were converted to concentration using the related calibration equations. The results obtained are summarized in Table 1. Application of the t-test at the 95% confidence level (with the critical t value of 2.27 for $n = 5$) indicates no statistically significant difference between the measured and actual concentration of analytes. However, the results show that the method has appropriate accuracy ($R\%$ is between 96.9 and 103.1) and precision ($RSD\%$ is in the range of 0.03 and 0.05).

The lifetime and Stability of the Proposed Sensor

The lifetime of the SY/NaOH-treated-GCE electrochemical sensor was evaluated with daily detection of analytical signals for three analytes for one week. For this purpose, the DPV analytical signals (Δi_p) of analytes were measured daily for a solution containing AA, DA, and UA with concentrations of 250.0, 15.0, and 20.0 μM , respectively, under the optimal conditions. After each daily

measurement, the electrode surface was first washed with distilled water and then placed in CBS pH = 5.0, and five potential cyclings were applied in the range of -0.5 to 1.5 V with a scan rate of 100 mV s^{-1} to clean the surface of the electrode. The cleaned electrode was kept in a glass tube for the subsequent experiments in the following days. The results show that the Δi_p of all three analytes was stable after one week, and only a 7% decrease in the analytical signals was observed during the seven repeated signal detection at one week.

The stability of the sensor response was also studied by about 60 sequential detections of analytical signals of analytes. The results obtained showed that after about 55 consecutive measurements of analytical signals in a CBS with a pH of 5.0, the analytical signals for three analytes are about 95% of the first recorded analytical signal, which confirms the excellent stability of the proposed sensor.

Repeatability and Reproducibility

Three SY/NaOH-treated-GCE sensors were constructed on three different days under optimum conditions and used to test sensor repeatability and reproducibility. Each electrode was subjected to four repeated DPV measurements of analytical signals. The obtained data is summarized in Table 2. Applying the analysis of variance (ANOVA) test to the data shows calculated F -values of 0.62, 0.9, and 0.5 for AA, DA, and UA, respectively, which are smaller than the critical F -value of 4.25 at the 95% confidence level. The three-day-made sensors exhibit good levels of repeatability and reproducibility in their responses, with a confidence level of 95%.

Interference Studies

Sensor selectivity is another important factor in the

Table 1. Accuracy and Precision Results for Simultaneous Determination of AA, DA, and UA with SY/NaOH-Treated-GCE

No.	Added (μM)			Founded (μM)			Recovery (%)			RSD		
	AA	DA	UA	AA	DA	UA	AA	DA	UA	AA	DA	UA
1	15.0	2.0	2.0	15.2	2.0	2.0	101.3	100.0	101.1	0.04	0.04	0.05
2	100.0	8.0	10.0	96.9	8.2	9.9	96.9	103.1	99.4	0.05	0.05	0.04
3	170.0	15.0	20.0	172.5	15.3	20.1	101.5	101.9	100.5	0.03	0.04	0.05

Table 2. Repeatability and Reproducibility Results for Simultaneous Determination of AA (150 μM), DA (5 μM), and UA (8 μM) in 4 ml CBS pH = 5 at SY/NaOH-treated-GCE

Modified electrode	Mean analytical signal (μM) \pm standard deviation		
	UA	DA	AA
The first electrode	5.3 \pm 0.1	3.5 \pm 0.2	2.6 \pm 0.2
The second electrode	5.4 \pm 0.2	3.3 \pm 0.4	2.3 \pm 0.6
The third electrode	5.4 \pm 0.4	3.6 \pm 0.2	2.4 \pm 0.3

Table 3. Investigating the Effect of Interferences on DPV Current for Simultaneous Determination of 20 μM , AA, and 5 μM , of Both DA and UA, Respectively

Coexisting species	Tolerance concentration AA or DA, or UA (μM)
Glucose, Fructose, Saccharose, Urea, EDTA, L-Alanine, NO_3^- , SO_4^{2-} , F^- , ClO_4^- , NH_4^+ , Li^+ , Ca^{2+} , Ba^{2+}	20000
Cl^-	15000
SCN^-	14000
CO_3^{2-}	11000
Vitamin B1	1200
CN^-	1000
Thiourea	500
Cefixime	400
Vitamin B6	200

simultaneous electrochemical measurement of analytes, especially in biological samples and in the presence of bioactive species. Therefore, to investigate the effect of the presence of different species in AA, DA, and UA measurements, five repeated DPV measurements of solutions containing specific concentrations of analytes (20 μM of AA, and 5 μM , of both DA and UA, respectively) were performed by SY/NaOH-treated-GCE under optimal conditions. In the absence of the interference species, the mean (\bar{X}) and standard deviation (S) of the analytical signals were calculated. Then known amounts of the interference species were added to the solution containing the analytes, and their analytical signal was recorded in the presence of the interference. If the analytical signals measured in the presence of interference are within the range of $\bar{X} \pm 3S$, the added species has not interfered in the simultaneous

determination. The results are presented in Table 3. As can be seen, numerous species do not affect the analyte signal measurement, confirming the selectivity of the method.

Real Sample Analysis

The application of the SY/NaOH-treated-GCE sensor in the routine analysis was validated by detecting the concentration of AA, DA, and UA in real samples such as water, bell peppers, grapefruit, and vitamin C tablets, and dopamine hydrochloride ampoules, urine, and human blood serum samples. After preparing real samples, a 2 ml of the aliquot of bell pepper and grapefruit sample and a 1 ml of the aliquot of tap water, urine, blood, dopamine injection, and vitamin C tablet sample were used to determine AA, DA, and UA according to the analytical procedure by applying the standard addition method.

Table 4. Results for AA, DA, and UA Determination in Different Real Samples were Obtained by the Proposed Method under the Optimum Conditions

Sample	Added (μM)			Found (μM) \pm SD (n = 3)			Recovery (%)			The analyte amount listed on the label	The calculated analyte amount \pm SD (n = 3)
	AA	DA	UA	AA	DA	UA	AA	DA	UA		
Dopamine injection	0.0	0.0	0.0	N.D	2.1 \pm 0.4	ND	ND	-	ND	40.0 mg ml ⁻¹	40.9 \pm 2.2 mg ml ⁻¹
	10.0	2.0	2.0	10.7 \pm 0.5	3.9 \pm 0.5	2.0 \pm 0.05	107.0	101.4	100.4		
	45.0	8.0	8.0	46.2 \pm 0.6	9.8 \pm 0.7	8.1 \pm 0.04	102.8	99.3	101.6		
	110.0	12.0	12.0	110.2 \pm 0.8	13.8 \pm 0.4	11.8 \pm 0.04	100.2	99.6	98.7		
vitamin C tablet	0.0	0.0	0.0	6.1 \pm 0.5	ND	ND	-	ND	ND	0.121 g g ⁻¹	0.118 \pm 0.01 g g ⁻¹
	10.0	2.0	2.0	21.6 \pm 0.7	2.1 \pm 0.5	2.0 \pm 0.6	103.8	104.8	99.2		
	45.0	8.0	8.0	56.7 \pm 1.5	8.2 \pm 0.8	8.3 \pm 0.5	101.7	102.0	103.7		
	110.0	12.0	12.0	124.4 \pm 0.5	11.6 \pm 0.5	11.7 \pm 0.4	103.8	96.9	97.6		
Tap water	0.0	0.0	0.0	N.D	N.D	N.D	N.D	N.D	N.D		
	10.0	2.0	2.0	10.7 \pm 0.5	2.1 \pm 0.4	1.9 \pm 0.4	107.5	107.7	101.9		
	45.0	8.0	8.0	46.7 \pm 0.4	8.2 \pm 0.3	8.1 \pm 0.4	103.8	102.0	101.3		
	110.0	12.0	12.0	109.3 \pm 0.4	11.9 \pm 0.4	12.1 \pm 0.3	99.3	99.2	101.2		
Bell pepper	0.0	0.0	0.0	42.4 \pm 0.4	ND	ND	-	ND	ND		
	10.0	2.0	2.0	58.6 \pm 0.5	2.1 \pm 0.5	2.00 \pm 0.5	99.04	107.1	100.4		
	45.0	8.0	8.0	95.0 \pm 0.4	8.1 \pm 0.5	8.05 \pm 0.4	103.9	101.0	100.6		
	110.0	12.0	12.0	159.5 \pm 0.5	12.2 \pm 0.5	12.4 \pm 0.4	101.6	101.8	103.7		
Grapefruit	0.0	0.0	0.0	20.6 \pm 0.6	ND	ND	-	ND	ND		
	10.0	2.0	2.0	36.5 \pm 0.4	2.2 \pm 0.45	2.0 \pm 0.4	108.9	108.4	101.0		
	45.0	8.0	8.0	71.4 \pm 0.5	8.2 \pm 0.5	8.3 \pm 0.5	101.7	103.2	103.6		
	110.0	12.0	12.0	136.8 \pm 0.6	12.6 \pm 0.5	12.4 \pm 0.4	101.1	104.7	103.7		
Human serum	0.0	0.0	0.0	ND	ND	0.67 \pm 0.83	ND	ND	-		
	10.0	2.0	2.0	10.7 \pm 0.5	2.1 \pm 0.4	2.4 \pm 0.4	107.0	107.1	97.9		
	45.0	8.0	8.0	46.7 \pm 0.6	8.01 \pm 0.7	8.5 \pm 0.5	103.8	100.2	100.5		
	110.0	12.0	12.0	111.6 \pm 0.5	12.4 \pm 0.5	12.6 \pm 0.8	101.5	103.6	101.4		
Human urine	0.0	0.0	0.0	N.D	N.D	2.8 \pm 0.7	ND	ND	-		
	10.0	2.0	2.0	10.6 \pm 0.4	2.1 \pm 0.8	4.5 \pm 0.4	106.5	107.7	99.2		
	45.0	8.0	8.0	46.2 \pm 0.5	8.0 \pm 0.5	10.4 \pm 0.7	102.8	100.2	98.0		
	110.0	12.0	12.0	109.7 \pm 0.5	12.4 \pm 0.6	15.0 \pm 0.4	99.8	103.6	103.5		

The dopamine amount listed on the ampoule label is 200 mg/5 ml. The amount of vitamin C listed on the pill label is 500 mg/4 g.

Then the real samples were spiked with specific and different volumes of standard samples AA, DA, and UA and tested by the proposed method. According to Table 4, the obtained recovery from the Spike method is in the range of 96.95-108.91. The results show that the SY/NaOH-treated-

GCE is suitable for measuring AA, DA, and UA. In addition, the amount of AA measured in vitamin C tablets and the amount of DA measured in dopamine injections according to the t-test at a 95% confidence level were not significantly different from the amounts indicated on the packaging of

Table 5. Comparison of SY/NaOH-Treated-GCE for the Determination of AA, DA, and UA with Previously Reported Ones

Electrode materials	Method	The detection limit			Linear range			Real sample	Ref.
		(μM)			(μM)				
		AA	DA	UA	AA	DA	UA		
C ₃ F ₇ -azo ⁺ /RGO/GCE	DPV	0.008	0.065	0.011	0.04-6.01	57.28-134.28	9.23-23.45	human serum	[107]
HNGA/GCE	DPV	16.7	0.22	0.12	50-1500	5-50	5-50	human urine	[108]
rGo/pd@ppy nps/GCE	DPV	0.049	0.056	0.047	38-1647	1.4-219	1.4-219	human serum	[109]
ZnCl ₂ -CF/GCE	DPV	0.02	0.16	0.11	0.05-200	2-2000	1-2500	human urine	[110]
SPES-SWCNT/GCE	DPV	10.6	0.015	0.113	200-1600	5.0-50	5.0-60	vitamin C tablets and DA injection	[111]
G-30	CV	17.8	1.44	0.29	50-1000	3-140	0.5- 150	vitamin C and DA hydrochloride tablet	[112]
Fe ₃ O ₄ @Au-Cys/PANI/GFE ^e	DPV	3.20	2.19	1.80	20-700	20-1,000	20-1,000	dopamine hydrochloride solution	[113]
SY/NaOH-treated-GCE	DPV	4.78	0.12	0.12	7-320	0.2-45	0.2-50	human urine Pimento Grapefruit Dopamine injection human serum human urine Tap water	This work

C₃F₇-azo⁺/RGO: polyfluorinated azobenzene/reduced graphene oxide nanocomposite. HNGA: holey nitrogen-doped graphene aerogel. rGo/pd@ppy nps: palladium nanoparticles supported on polypyrrole/reduced graphene oxide. ZnCl₂-CF: zinc chloride nanoparticles- kiwi skin-derived microporous carbons electrochemical sensor. SPES-SWCNT/GCE: sulfonated poly (ether sulfone)-single-walled carbon nanotubes/glassy carbon electrode. G-30: graphene ink coated glass. Fe₃O₄@Au-Cys/PANI/GFE: Magnetite nanoparticle@ conjugated gold-coated based on cysteine/polyaniline/ modified graphite electrodes.

these samples, which indicates the accuracy of the method.

CONCLUSIONS

In this report, for the first time, the GC electrode was modified using a simple, environmentally friendly, and inexpensive Sunset Yellow modifier. The SY/NaOH-treated-GCE was characterized by EIS, chronoamperometry, chronocoulometry, and CV. The collected data demonstrate that electrochemical treatment of GCE with SY/NaOH increases its active surface area, lifetime, stability, and electrical conductivity. Also, the appropriate electrocatalytic response with significant peak separation in the simultaneous electrochemical oxidation of AA, DA, and UA on the surface of the SY/NaOH-treated-GCE indicates that this modified electrode is a suitable sensor for practical applications. The modified electrode for measuring AA, DA, and UA showed excellent recovery (96.95-108.91) in real samples such as

bell peppers, grapefruit, dopamine ampoules, vitamin C pills, urine, and blood serum. Due to the efficiency of the electrode in the numerous real samples, the SY/NaOH-treated-GCE provides an efficient analytical utility for on-site biologic analysis and food safety monitoring. In comparison to other sensors (HNGA/GCE, SPES-SWCNT/GCE, G-30, Fe₃O₄@Au-Cys/PANI/GFE) reported by the researchers in Table 5, our sensor has a high figure of merit due to its low detection limits of 4.78 M, 0.12 M, and 0.12 M, respectively. Moreover, the proposed sensor has a more straightforward and faster modification method than C₃F₇-azo⁺/RGO/GCE and ZnCl₂-CF/GCE sensors.

REFERENCES

- [1] M.W. Davey, M.V. Montagu, D. Inze, M. Sanmartin, A. Kanellis, N. Smirnoff, I.J.J. Benzie, J.J. Strain, D. Favell, J. Fletcher, *J. Sci. Food Agric.* 80 (2000) 825.

- [2] M. Attia, E.A. Essa, R.M. Zaki, A.A. Elkordy, *Antioxidants* 9 (2020) 359.
- [3] S.J. Ballaz, G.V. Rebec, *Pharmacol. Res.* 146 (2019) 104321.
- [4] J. Reang, P.C. Sharma, V.K. Thakur, J. Majeed, *Biomolecules* 11 (2021) 1130.
- [5] W.V.B. Robertson, B. Schwartz, *J. Biol. Chem.* 201 (1953) 689.
- [6] H. Brise, L. Hallberg, *J. Intern. Med.* 171 (1962) 51.
- [7] M. Sabatier, A. Rytz, J. Husny, S. Dubascoux, M. Nicolas, A. Dave, H. Singh, M. Bodis, R.P. Glahn, *Nutrients* 12 (2020) 2776.
- [8] R.E. Hodges, J. Hood, J.E. Canham, H.E. Sauberlich, E.M. Baker, *Am. J. Clin. Nutr.* 24 (1971) 432.
- [9] L. Maxfield, J.S. Crane (2018).
- [10] S.J. Padayatty, A. Katz, Y. Wang, P. Eck, O. Kwon, J.-H. Lee, S. Chen, C. Corpe, A. Dutta, S.K. Dutta, J. *Am. Coll. Nutr.* 22 (2003) 18.
- [11] K. Gillis, K.K. Stevens, E. Bell, R.K. Patel, A.G. Jardine, S.T. Morris, M.P. Schneider, C. Delles, P.B. Mark, *Clinical Kidney Journal* 11 (2018) 532.
- [12] A. Sorice, E. Guerriero, F. Capone, G. Colonna, G. Castello, S. Costantini, *Mini Rev. Med. Chem.* 14 (2014) 444.
- [13] D. Jafari, A. Esmaeilzadeh, M. Mohammadi-Kordkhayli, N. Rezaei, *Vitamin C and the immune system*, in: *Nutrition and Immunity*, Springer, 2019, pp. 81-102.
- [14] J.A. Olson, R.E. Hodges, *Am. J. Clin. Nutr.* 45 (1987) 693.
- [15] S. McLennan, D.K. Yue, E. Fisher, C. Capogreco, S. Heffernan, G.R. Ross, J.R. Turtle, *Diabetes* 37 (1988) 359.
- [16] I.B. Hirsch, D.H. Atchley, E. Tsai, R.F. Labbe, A. Chait, *J. Diabetes Complications* 12 (1998) 259.
- [17] T. Riemensperger, G. Isabel, H. Coulom, K. Neuser, L. Seugnet, K. Kume, M. Iché-Torres, M. Cassar, R. Strauss, T. Preat, *Proceedings of the National Academy of Sciences* 108 (2011) 834.
- [18] M. Li, L. Zhou, X. Sun, Y. Yang, C. Zhang, T. Wang, F. Fu, *Biomed. Pharmacother.* 145 (2022) 112458.
- [19] R. Franco, I. Reyes-Resina, G. Navarro, *Biomedicines* 9 (2021) 109.
- [20] A.F. Leentjens, *Drugs* 71 (2011) 273.
- [21] M.-J. Ribeiro, M. Vidailhet, C. Loc'h, C. Dupel, J.P. Nguyen, M. Ponchant, F. Dollé, M. Peschanski, P. Hantraye, P. Cesaro, *Arch. Neurol.* 59 (2002) 580.
- [22] Y.S. Oh, J.S. Kim, S.W. Yoo, E.J. Hwang, C. Lyoo, K.S. Lee, *Eur. J. Neurol.* 27 (2020) 258.
- [23] S. Capellino, K. Frommer, M. Rickert, J. Steinmeyer, S. Rehart, U. Müller-Ladner, E. Neumann, OP0149 Dopamine Pathway and Bone Metabolism in Rheumatoid Arthritis, in: *BMJ Publishing Group Ltd.*, 2016.
- [24] R. Brisch, A. Saniotis, R. Wolf, H. Biela, H.-G. Bernstein, J. Steiner, B. Bogerts, K. Braun, Z. Jankowski, J. Kumaratilake, *Frontiers in Psychiatry* 5 (2014) 47.
- [25] C. Landvogt, H.G. Buchholz, V. Bernedo, M. Schreckenberger, K.J. Werhahn, *Epilepsia* 51 (2010) 1699.
- [26] L. Rocha, M. Alonso-Vanegas, J. Villeda-Hernández, M. Mújica, J.M. Cisneros-Franco, M. López-Gómez, C. Zavala-Tecuapetla, C.L. Frías-Soria, J. Segovia-Vila, A. Borsodi, *Neurobiol. Dis.* 45 (2012) 499.
- [27] Y. Ito, Y. Fuimoto, T. Obara, *World J. Surg.* 16 (1992) 759.
- [28] T.N. Weingarten, T.L. Welch, T.L. Moore, G.F. Walters, J.L. Whipple, A. Cavalcante, I. Bancos, W.F. Young, Jr., L.M. Gruber, M.Z. Shah, T.J. McKenzie, D.R. Schroeder, *J. Sprung, Urology* 100 (2017) 131.
- [29] M.R. Moghadam, S. Dadfarnia, A.M.H. Shabani, P. Shahbazikhah, *Anal. Biochem.* 410 (2011) 289.
- [30] R. Ojani, J.-B. Raouf, E. Zarei, S.N. Azizi, M. Abrishamkar, *Monatshfte für Chemie-Chemical Monthly* 143 (2012) 7.
- [31] Y.L. Jin, T. Zhu, L. Xu, W.S. Zhang, B. Liu, C.Q. Jiang, H. Yu, L.M. Huang, K.K. Cheng, G.N. Thomas, T.H. Lam, *Int. J. Cardiol.* 168 (2013) 2238.
- [32] X. Liu, P.B. Lillehoj, *Biosens. Bioelectron.* 98 (2017) 189.
- [33] P. Fang, X. Li, J.J. Luo, H. Wang, X.-F. Yang, *Brain Disorders & Therapy* 2 (2013) 109.
- [34] C. Borghi, E.A. Rosei, T. Bardin, J. Dawson, A. Dominiczak, J.T. Kielstein, A.J. Manolis, F. Perez-Ruiz, G. Mancia, *J. Hypertens.* 33 (2015) 1729.
- [35] D. He, Z. Zhang, Y. Huang, Y. Hu, H. Zhou, D. Chen, *Luminescence* 20 (2005) 271.

- [36] H. Khajehsharifi, E. Pourbasheer, H. Tavallali, S. Sarvi, M. Sadeghi, Arab. J. Chem. 10 (2017) S3451.
- [37] G.E. De Benedetto, D. Fico, A. Pennetta, C. Malitesta, G. Nicolardi, D.D. Lofrumento, F. De Nuccio, V. La Pesa, J. Pharm. Biomed. Anal. 98 (2014) 266.
- [38] H.-B. Wang, H.-D. Zhang, Y. Chen, K.-J. Huang, Y.-M. Liu, Sensors Actuators B: Chem. 220 (2015) 146.
- [39] D. Jin, M.-H. Seo, B.T. Huy, Q.-T. Pham, M.L. Conte, D. Thangadurai, Y.-I. Lee, Biosens. Bioelectron. 77 (2016) 359.
- [40] R. Liu, R. Yang, C. Qu, H. Mao, Y. Hu, J. Li, L. Qu, Sensors Actuators B: Chem. 241 (2017) 644.
- [41] R.A. Thearle, N.M. Latiff, Z. Sofer, V. Mazánek, M. Pumera, Electroanalysis 29 (2017) 45.
- [42] S.I. Kaya, S. Kurbanoglu, S.A. Ozkan, Crit. Rev. Anal. Chem. 49 (2019) 101.
- [43] M. Nemakal, S. Aralekallu, I. Mohammed, K.P. CP, L.K. Sannegowda, Microchem. J. 143 (2018) 82.
- [44] Ö. Güngör, O. Özgül, B. Aksoy, F. Okuşluk, S. Köytepe, Polym. Bull. (2022) 1.
- [45] K.P. Aryal, H.K. Jeong, Chem. Phys. Lett. 768 (2021) 138405.
- [46] H. Beitollahi, M. Safaei, S. Tajik, Anal. Bioanal. Chem. Res. 6 (2019) 81.
- [47] D. Jia, J. Dai, H. Yuan, L. Lei, D. Xiao, Talanta 85 (2011) 2344.
- [48] Q. Zhu, J. Bao, D. Huo, M. Yang, C. Hou, J. Guo, M. Chen, H. Fa, X. Luo, Y. Ma, Sensors Actuators B: Chem. 238 (2017) 1316.
- [49] R. Li, T. Yang, Z. Li, Z. Gu, G. Wang, J. Liu, Anal. Chim. Acta 954 (2017) 43.
- [50] T. Madrakian, E. Haghshenas, A. Afkhami, Sensors Actuators B: Chem. 193 (2014) 451.
- [51] X. Niu, W. Yang, H. Guo, J. Ren, F. Yang, J. Gao, Talanta 99 (2012) 984.
- [52] H. Bagheri, N. Pajooheshpour, B. Jamali, S. Amidi, A. Hajian, H. Khoshshafar, Microchem. J. 131 (2017) 120.
- [53] B. Dinesh, V. Veeramani, S.-M. Chen, R. Saraswathi, J. Electroanal. Chem. 786 (2017) 169.
- [54] M. Sajid, M.K. Nazal, M. Mansha, A. Alsharaa, S.M.S. Jillani, C. Basheer, TrAC, Trends Anal. Chem. 76 (2016) 15.
- [55] M.A. Rather, S.A. Bhat, S.A. Pandit, G.M. Rather, K.Z. Khan, M.A. Bhat, Electroanalysis 29 (2017) 1772.
- [56] F.R. Caetano, L.B. Felipe, A.J.G. Zarbin, M.F. Bergamini, L.H. Marcolino-Junior, Sensors Actuators B: Chem. 243 (2017) 43.
- [57] A.A. Abdelwahab, Y.-B. Shim, Sensors Actuators B: Chem. 221 (2015) 659.
- [58] X. Ma, M. Chao, Z. Wang, Analytical Methods 4 (2012) 1687.
- [59] M.M. Rahman, N.S. Lopa, M.J. Ju, J.-J. Lee, J. Electroanal. Chem. 792 (2017) 54.
- [60] Q. Lian, Z. He, Q. He, A. Luo, K. Yan, D. Zhang, X. Lu, X. Zhou, Anal. Chim. Acta 823 (2014) 32.
- [61] P.K. Aneesh, S.R. Nambiar, T.P. Rao, A. Ajayaghosh, Analytical Methods 6 (2014) 5322.
- [62] A. Ejaz, Y. Joo, S. Jeon, Sensors Actuators B: Chem. 240 (2017) 297.
- [63] M. Wang, H. Guo, N. Wu, J. Zhang, T. Zhang, B. Liu, Z. Pan, L. Peng, W. Yang, Colloids Surf. Physicochem. Eng. Aspects 634 (2022) 127928.
- [64] H. Daneshinejad, M.A. Chamjangali, N. Goudarzi, A. Roudbari, Materials Science and Engineering: C 58 (2016) 532.
- [65] A. Özcan, S. İlkbaş, A. Atılır Özcan, Talanta 165 (2017) 489.
- [66] D. Zhang, L. Li, W. Ma, X. Chen, Y. Zhang, Materials Science and Engineering: C 70 (2017) 241.
- [67] M. Arab Chamjangali, A.A. Reskety, N. Goudarzi, G. Bagherian, Electroanalysis 27 (2015) 2708.
- [68] A. Hatefi-Mehrjardi, N. Ghaemi, M.A. Karimi, M. Ghasemi, S. Islami-Ramchahi, Electroanalysis 26 (2014) 2491.
- [69] S. Yang, G. Li, R. Yang, M. Xia, L. Qu, J. Solid State Electrochem. 15 (2011) 1909.
- [70] M.C. Henstridge, E.J. Dickinson, M. Aslanoglu, C. Batchelor-McAuley, R.G. Compton, Sensors Actuators B: Chem. 145 (2010) 417.
- [71] R. Zhang, S. Liu, L. Wang, G. Yang, Measurement 46 (2013) 1089.
- [72] Y. Zhou, W. Tang, J. Wang, G. Zhang, S. Chai, L. Zhang, T. Liu, Analytical Methods 6 (2014) 3474.
- [73] X.-B. Li, M.M. Rahman, C.-Y. Ge, G.-R. Xu, J.-J. Lee, J. Electrochem. Soc. 164 (2017) B34.
- [74] M.B. Gholivand, Y. Yamini, M. Dayeni, S. Seidi, E. Tahmasebi, Journal of Environmental Chemical Engineering 3 (2015) 529.

- [75] D.R. Lima, L. Klein, G.L. Dotto, *Environmental Science and Pollution Research* 24 (2017) 21484.
- [76] L. Chen, Y. Li, Q. Du, Z. Wang, Y. Xia, E. Yedinak, J. Lou, L. Ci, *Carbohydr. Polym.* 155 (2017) 345.
- [77] S.H. Chen, A.S.Y. Ting, *Microfungi for the Removal of Toxic Triphenylmethane Dyes*, in: *Mining of Microbial Wealth and MetaGenomics*, Springer, 2017, pp. 405-429.
- [78] T. Del Giacco, R. Germani, F. Saracino, M. Stradiotto, *J. Photochem. Photobiol. A: Chem.* 332 (2017) 546.
- [79] M. Bilal, T. Rasheed, H.M. Iqbal, C. Li, H. Wang, H. Hu, W. Wang, X. Zhang, *Chem. Eng. Res. Des.* 129 (2018) 384.
- [80] H. Nadaroglu, S. Cicek, A.A. Gungor, *Spectrochimica Acta Part A: Molecular and Biomolecular Spectroscopy* 172 (2017) 2.
- [81] P.S. Ganesh, BE Kumara Swamy, *J. Electroanal. Chem.* 756 (2015) 193.
- [82] P. Ganesh, K.B. Swamy, *Journal of Analytical & Bioanalytical Techniques* 6 (2015) 1.
- [83] P. Ganesh, B.K. Swamy, *Journal of Analytical & Bioanalytical Techniques* 6 (2015) 1.
- [84] J.B. G H Jeffery, J. Mendham, R.C. Denney, *vogel's Textbook of Quantitative Chemical Analysis* 5th.ed. Page 289, 5 ed., Longman Scientific & Technical, 1989.
- [85] P. Sierra-Rosales, C. Berríos, S. Miranda-Rojas, J.A. Squella, *Electrochim. Acta* 290 (2018) 556.
- [86] A.M.M. Durigon, G.D. da Silveira, F.R. Sokal, R.A.C.V. Pires, D. Dias, *J. Solid State Electrochem.* 24 (2020) 2907.
- [87] L. Zhang, Y. Sun, X. Lin, *Analyst* 126 (2001) 1760.
- [88] C.A. Martínez-Huitle, M. Cerro-Lopez, M.A. Quiroz, *Mater. Res.* 12 (2009) 375.
- [89] G. Shul, M. Weissmann, D. Bélanger, *Langmuir* 30 (2014) 6612.
- [90] X. Li, Y. Wan, C. Sun, *J. Electroanal. Chem.* 569 (2004) 79.
- [91] G. Yang, B. Liu, S. Dong, *J. Electroanal. Chem.* 585 (2005) 301.
- [92] A.J. Bard, L.R. Faulkner, *Electrochemical Methods* 2 (2001) 580.
- [93] F.C. Anson, *Anal. Chem.* 38 (1966) 54.
- [94] E. Laviron, L. Roullier, R. Gavasso, *J. Electroanal. Chem. Interf. Electrochem.* 75 (1977) 287.
- [95] C.G. Heald, G.G. Wildgoose, L. Jiang, T.G. Jones, R.G. Compton, *Chemphyschem* 5 (2004) 1794.
- [96] H.C. Leventis, I. Streeter, G.G. Wildgoose, NS. Lawrence, L. Jiang, T.G. Jones, R.G. Compton, *Talanta* 63 (2004) 1039.
- [97] C. Wang, C. Li, F. Wang, C. Wang, *Microchimica Acta* 155 (2006) 365.
- [98] R. Reeves, AM Bond, *Modern Polarographic Methods in Analytical Chemistry*, Marcel Dekker, New York and Basel (1980), 518 pp., Sfr. 135.00, in, Elsevier, 1980, pp. 29-30.
- [99] A.P. Brown, F.C. Anson, *Anal. Chem.* 49 (1977) 1589.
- [100] J.C. Myland, K.B. Oldham, *Electrochem. Commun.* 7 (2005) 282.
- [101] A. Dekanski, J. Stevanović, R. Stevanović, B.Ž. Nikolić, V.M. Jovanović, *Carbon* 39 (2001) 1195.
- [102] B. Habibi, M.H. Pournaghi-Azar, *Electrochim. Acta* 55 (2010) 5492.
- [103] L. Zhang, J. Lian, *J. Electroanal. Chem.* 611 (2007) 51.
- [104] I.F. Hu, T. Kuwana, *Anal. Chem.* 58 (1986) 3235.
- [105] P. Karabinas, D. Jannakoudakis, *J. Electroanal. Chem. Interf. Electrochem.* 160 (1984) 159.
- [106] J.-L. Wang, B.-C. Li, Z.-J. Li, K.-F. Ren, L.-J. Jin, S.-M. Zhang, H. Chang, Y.-X. Sun, J. Ji, *Biomaterials* 35 (2014) 7679.
- [107] S. Wu, H. Wang, B. Zhao, T. Cao, J. Ma, L. Liu, Z. Tong, *Talanta* 237 (2022) 122986.
- [108] S. Feng, L. Yu, M. Yan, J. Ye, J. Huang, X. Yang, *Talanta* 224 (2021) 121851.
- [109] B. Demirkan, S. Bozkurt, K. Cellat, K. Arıkan, M. Yılmaz, A. Şavk, M.H. Çalmlı, M.S. Nas, M.N. Atalar, M.H. Alma, F. Sen, *Sci. Rep.* 10 (2020) 2946.
- [110] W. Zhang, L. Liu, Y. Li, D. Wang, H. Ma, H. Ren, Y. Shi, Y. Han, B.-C. Ye, *Biosens. Bioelectron.* 121 (2018) 96.
- [111] D. Thirumalai, D. Subramani, J.-H. Yoon, J. Lee, H.-J. Paik, S.-C. Chang, *New J. Chem.* 42 (2018) 2432.
- [112] L. Fu, A. Wang, G. Lai, W. Su, F. Malherbe, J. Yu, C.-T. Lin, A. Yu, *Talanta* 180 (2018) 248.
- [113] N. Nontawong, M. Amatatongchai, W. Wuepchaiyaphum, S. Chairam, S. Pimmongkol, S. Panich, S. Tamuang, P. Jarujamrus, *Int. J. Electrochem. Sci.* 13 (2018) 6940.